Sensitivity Methods in the Dispatch and Siting of FACTS Controllers

Xinghao Fang, Joe H. Chow, Xia Jiang, Bruce Fardanesh, Edvina Uzunovic, and Abdel-Aty Edris

***Abstract*—Flexible ac Transmission Systems (FACTS) play an important role in improving the transfer capability and stability of a power system. In the application of voltage-sourced converter (VSC)-based FACTS controllers, it is important to study how a VSC impacts the flows in a power system. In this paper, we investigate this flow control problem using two sensitivity approaches, one using an injected voltage source formulation and the other an equivalent impedance formulation. The applications of sensitivity analysis for line active power redispatch and for new series VSC siting in a 1673-bus system are presented.**

***Index Terms*—Equivalent impedance, FACTS controllers, sensitivity analysis, voltage source model, voltage-sourced converter.**

I. Introduction

FLEXIBLE ac transmission systems (FACTS), which are based on power electronic devices, have the capability to enhance the stability and transfer capability of existing ac networks. These high-voltage, high-current power electronic devices can be configured into a family of voltage-sourced converter (VSC)-based FACTS controllers which have been systematically developed and installed for industrial applications. These controllers include static synchronous compensators (STATCOM) [1], back-to-back STATCOMs (BtB STATCOM) [2], static synchronous series compensators (SSSC) [3], unified power flow controllers (UPFC) [4], interline power flow controllers (IPFC) [5], generalized unified power flow controllers (GUPFC) [6], and convertible series compensators (CSC) [7].

In the operation of VSC-based FACTS controllers in a large power system, it is desirable to have a systematic and efficient tool to investigate how the VSCs can impact the operation of the whole system. Sensitivity analysis is often used for this purpose, because it sets up a direct analytical relation between the control variables and observed variables, like line power flows and bus voltages. Such relations are useful for many practical applications, including real-time dispatch of the series VSC to relieve line overload, which has been practiced by New York Power Authority (NYPA) and New York Independent System Operator (NYISO).

Various sensitivity approaches, including those in [8]–[13], have been proposed for FACTS controllers. In this paper, we investigate the sensitivities of the active power flow and voltage response due to the voltage injection from VSCs, and propose two sensitivity analysis methods. One approach is an analytical sensitivity formulation [14] with the VSC modeled as an injected voltage source [15]–[18]. This approach computes directly the incremental bus voltages and line flows from the perturbations of the VSC variables. The other approach is an indirect approach, which models the VSC as an equivalent impedance insertion [19], [20]. Then the sensitivity can be found by computing the variations of the network variables with respect to line impedance perturbations. Both approaches are first-order linear expansions and can provide approximate solutions without extensive computation. The indirect method has the advantage of including the effect of a FACTS controller in the power system, without actually building a FACTS controller model. Thus it is especially suitable for the sensitivity computation of FACTS controllers in a large number of locations. The sensitivity algorithm has been incorporated in the EPRI/NYPA FACTS Controller Operator Training Simulator [21] and applied to a 1673-bus power system. The analytical sensitivity method is illustrated in two practical applications for shifting line flows using a UPFC and two separate SSSCs. The equivalent impedance method is illustrated as a series VSC siting problem.

This paper is organized as follows. Sections II and III introduce the injected-voltage-source-model-based and equivalent-reactance-model-based sensitivity formulations, respectively. The practical applications of sensitivities in a 1673-bus system [22] are discussed in Section IV. The conclusion is summarized in Section V.

II. Voltage Source Model-Based Sensitivity Analysis

A. Voltage Source Model and Sensitivities

With this method, a VSC is modeled as an injected voltage source. As an example, consider a UPFC applied to the system in Fig. 1(a), where the series VSC is inserted between Buses 1 and 2. The circuit representation is shown in Fig. 1(b), where the shunt voltage insertion is $\tilde{V}_{m1} = V_{m1}\varepsilon^{j\alpha_1}$ and the series voltage insertion is $\tilde{V}_{m2} = V_{m1}\varepsilon^{j\alpha_2}$. The reactances X_{t1} and X_{t2} are the reactances of the shunt and series transformers, respectively, which are assumed to be lossless. When any one of the variables V_{m1}, α_1, V_{m2}, and α_2 are changed, all the state variables of the

Manuscript received November 11, 2008. First published March 31, 2009; current version published April 22, 2009. This work was supported by EPRI, NYPA, and the National Science Foundation under Grants ECS-0300025 and ECS-0622119. Paper no. TPWRS-00810-2007.

X. Fang was with Rensselaer Polytechnic Institute, Troy, NY 12180-3590 USA. He is now with the National Grid, Westborough, MA, 01582-0001 USA (e-mail: xinghao.fang@us.ngrid.com).

J. H. Chow is with Rensselaer Polytechnic Institute, Troy, NY 12180-3590 USA (e-mail: chowj@rpi.edu).

X. Jiang and B. Fardanesh are with the New York Power Authority, White Plains, NY 10601 USA.

E. Uzunovic is with Alliant Energy, Madison, WI 53707 USA.

A.-A. Edris is with Siemens-PTI, San Jose, CA 95101 USA.

Color versions of one or more of the figures in this paper are available online at http://ieeexplore.ieee.org.

Digital Object Identifier 10.1109/TPWRS.2009.2016531

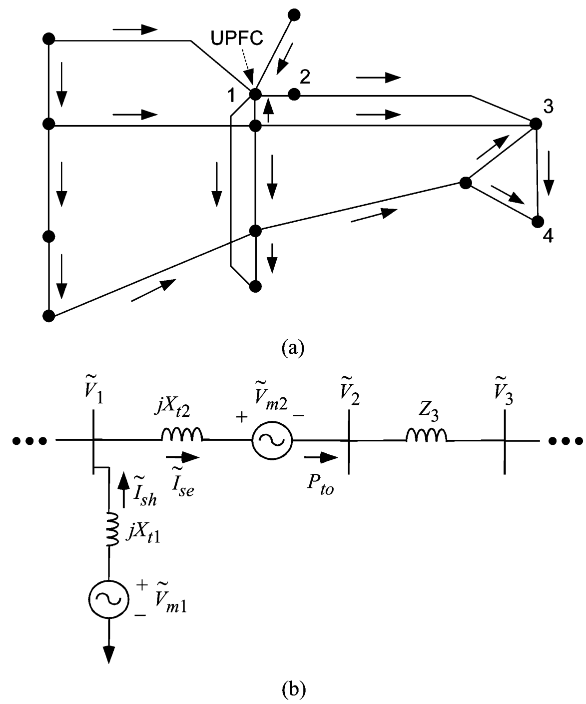

Fig. 1. Injected voltage source model for a UPFC. (a) System connection. (b) UPFC model.

system will change accordingly, affecting the power flow on all transmission lines.

For the line with series connected VSC, like the line from Bus 1 to Bus 2 in Fig. 1(b), the active power flow through the line is

$$P_{\text{to}} = \frac{V_2(V_{m2}\sin(\theta_2-\alpha_2) - V_1\sin(\theta_2-\theta_1))}{X_{t2}}. \quad (1)$$

If the perturbations ΔV_{m2} and $\Delta\alpha_2$ are introduced to the series voltage source, the variables of the adjacent buses will also be changed, which are denoted by ΔV_1, ΔV_2, $\Delta\theta_1$, and $\Delta\theta_2$. So the incremental line active power can be expressed as

$$\Delta P_{\text{to}} = G_{11}\begin{bmatrix}\Delta V_1\\ \Delta V_2\\ \Delta\theta_1\\ \Delta\theta_2\end{bmatrix} + G_{12}\begin{bmatrix}\Delta V_{m2}\\ \Delta\alpha_2\end{bmatrix} \quad (2)$$

where

$$G_{11} = \begin{bmatrix}\frac{\partial P_{\text{to}}}{\partial V_1} & \frac{\partial P_{\text{to}}}{\partial V_2} & \frac{\partial P_{\text{to}}}{\partial \theta_1} & \frac{\partial P_{\text{to}}}{\partial \theta_2}\end{bmatrix} \quad (3)$$

$$G_{12} = \begin{bmatrix}\frac{\partial P_{\text{to}}}{\partial V_{m2}} & \frac{\partial P_{\text{to}}}{\partial \alpha_2}\end{bmatrix} \quad (4)$$

$$\frac{\partial P_{\text{to}}}{\partial V_{m2}} = \frac{V_2\sin(\theta_2-\alpha_2)}{X_{t2}} \quad (5)$$

$$\frac{\partial P_{\text{to}}}{\partial \alpha_2} = -\frac{V_2V_{m2}\cos(\theta_2-\alpha_2)}{X_{t2}} \quad (6)$$

$$\frac{\partial P_{\text{to}}}{\partial V_1} = \frac{V_2\sin(\theta_1-\theta_2)}{X_{t2}} \quad (7)$$

$$\frac{\partial P_{\text{to}}}{\partial V_2} = \frac{V_{m2}\sin(\theta_2-\alpha_2) - V_1\sin(\theta_2-\theta_1)}{X_{t2}} \quad (8)$$

$$\frac{\partial P_{\text{to}}}{\partial \theta_1} = \frac{V_1V_2\cos(\theta_1-\theta_2)}{X_{t2}} \quad (9)$$

$$\frac{\partial P_{\text{to}}}{\partial \theta_2} = \frac{V_2V_{m2}\cos(\theta_2-\alpha_2) - V_1V_2\cos(\theta_2-\theta_1)}{X_{t2}}. \quad (10)$$

For other lines where there is no series VSC, like the line from Bus 3 to Bus 4, the line active power can be expressed as

$$P_\ell = \frac{V_3V_4[R_{34}\cos(\theta_3-\theta_4) + X_{34}\sin(\theta_3-\theta_4)] - R_{34}V_4^2}{R_{34}^2 + X_{34}^2} \quad (11)$$

where R_{34} and X_{34} are the line resistance and reactance, respectively. Denoting ΔV_3, ΔV_4, $\Delta\theta_3$, and $\Delta\theta_4$ as the perturbations arising from ΔV_{m2} and $\Delta\alpha_2$, the incremental line active power is

$$\Delta P_\ell = G_{21}\begin{bmatrix}\Delta V_3\\ \Delta V_4\\ \Delta\theta_3\\ \Delta\theta_4\end{bmatrix} \quad (12)$$

where

$$G_{21} = \begin{bmatrix}\frac{\partial P_\ell}{\partial V_3} & \frac{\partial P_\ell}{\partial V_4} & \frac{\partial P_\ell}{\partial \theta_3} & \frac{\partial P_\ell}{\partial \theta_4}\end{bmatrix} \quad (13)$$

$$\frac{\partial P_\ell}{\partial V_3} = \frac{V_4[R_{34}\cos(\theta_3-\theta_4) + X_{34}\sin(\theta_3-\theta_4)]}{R_{34}^2 + X_{34}^2} \quad (14)$$

$$\frac{\partial P_\ell}{\partial V_4} = \frac{V_3[R_{34}\cos(\theta_3-\theta_4) + X_{34}\sin(\theta_3-\theta_4)] - 2R_{34}V_4}{R_{34}^2 + X_{34}^2} \quad (15)$$

$$\frac{\partial P_\ell}{\partial \theta_3} = \frac{V_3V_4[X_{34}\cos(\theta_3-\theta_4) - R_{34}\sin(\theta_3-\theta_4)]}{R_{34}^2 + X_{34}^2} \quad (16)$$

$$\frac{\partial P_\ell}{\partial \theta_4} = \frac{V_3V_4[R_{34}\sin(\theta_3-\theta_4) - X_{34}\cos(\theta_3-\theta_4)]}{R_{34}^2 + X_{34}^2}. \quad (17)$$

Comparing (5), (6), (8), and (10) with (15) and (17) for a small line resistance, we can readily see the impact of the inserted voltage source variables V_{m2} and α_2 on the incremental line power flow.

B. Perturbation Analysis

To obtain the incremental line power flow solely as a function of ΔV_m and $\Delta\alpha$, we need the Jacobian matrix from the load-flow solution to eliminate the bus voltage perturbation variables. In an N-bus power network with N_g generators and M VSCs, the network equations can be formulated as $N-1$ equations for active power bus injections/loads P, $N-N_g$ equations of reactive power bus injections/loads Q, and $2M$ VSC equations, expressed as

$$\begin{bmatrix} P \\ Q \\ R \end{bmatrix} = \bar{f}(\bar{v}) = \begin{bmatrix} \bar{f}_P(\bar{v}) \\ \bar{f}_Q(\bar{v}) \\ \bar{f}_{\mathrm{VSC}}(\bar{v}) \end{bmatrix}, \bar{v} = \begin{bmatrix} V \\ \theta \\ V_m \\ \alpha \end{bmatrix} \tag{18}$$

where R is the vector of the VSC controller setpoints, and $\bar{v}$ is the vector of all the voltage variables of the network, including the variables of the FACTS controllers. The VSC setpoint equation (the third row) depends on the type and regulation mode of the FACTS controllers [22], [23].

At any operating condition $\bar{v}_0$ satisfying the bus power injections and VSC setpoints according to (18), the bus injection subject to small perturbations of $\bar{v}$ is given by (19). Given that the power injections are fixed, that is, $\Delta P = 0$ and $\Delta Q = 0$, the voltage variable perturbation can be solved from the VSC perturbation as in (20)

$$\begin{bmatrix} \Delta P \\ \Delta Q \end{bmatrix} = \left[\begin{array}{cc|cc} \partial \bar{f}_P/\partial V & \partial \bar{f}_P/\partial \theta & \partial \bar{f}_P/\partial V_m & \partial \bar{f}_P/\partial \alpha \\ \partial \bar{f}_Q/\partial V & \partial \bar{f}_Q/\partial \theta & \partial \bar{f}_Q/\partial V_m & \partial \bar{f}_Q/\partial \alpha \end{array}\right]_{\bar{v}=\bar{v}_0} \times \begin{bmatrix} \Delta V \\ \Delta \theta \\ \hline \Delta V_m \\ \Delta \alpha \end{bmatrix} \tag{19}$$

$$\begin{aligned} \begin{bmatrix} \Delta V \\ \Delta \theta \end{bmatrix} &= - \begin{bmatrix} \partial \bar{f}_P/\partial V & \partial \bar{f}_P/\partial \theta \\ \partial \bar{f}_Q/\partial V & \partial \bar{f}_Q/\partial \theta \end{bmatrix}^{-1}_{\bar{v}=\bar{v}_0} \\ &\quad \times \begin{bmatrix} \partial \bar{f}_P/\partial V_m & \partial \bar{f}_P/\partial \alpha \\ \partial \bar{f}_Q/\partial V_m & \partial \bar{f}_Q/\partial \alpha \end{bmatrix}_{\bar{v}=\bar{v}_0} \begin{bmatrix} \Delta V_m \\ \Delta \alpha \end{bmatrix} \\ &= G \begin{bmatrix} \Delta V_m \\ \Delta \alpha \end{bmatrix}. \end{aligned} \tag{20}$$

Finally, combining (2), (12), and (20), the incremental line active power flows are obtained as

$$\begin{bmatrix} \Delta P_{\mathrm{to}} \\ \Delta P_{\ell} \end{bmatrix} = (G_1 G_s + G_2) \begin{bmatrix} \Delta V_m \\ \Delta \alpha \end{bmatrix} \tag{21}$$

where

$$G_1 = \begin{bmatrix} G_{11} \\ G_{21} \end{bmatrix}, \quad G_2 = \begin{bmatrix} G_{12} \\ 0 \end{bmatrix} \tag{22}$$

and G_s denotes the rows of G in (20) corresponding to the incremental voltages and angles of the appropriate buses. We should note that in forming G_1 it may be necessary to introduce zero columns into G_{11} and G_{21}.

The purpose of this standard sensitivity derivation is to show the impact of the inserted voltage sources arising from FACTS controllers. The sensitivity (21) was computed in [18] using repeated loadflow solutions. Here we show the analytical expression for the sensitivity, which requires only the nominal loadflow solution. The analytical sensitivities hold when a VSC is operating within its rated limits and will be used to evaluate the accuracy of the equivalent impedance method presented in the next section.

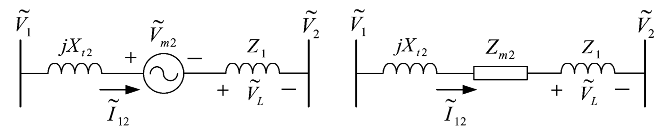

Fig. 2. SSSC model. (a) Voltage source model. (b) Equivalent impedance model.

III. Equivalent Impedance-Based Sensitivity Analysis

A. Equivalent Impedance Model of VSCs

When a VSC is inserted into a system, the voltage source injected by the VSC can be treated as an equivalent impedance without changing the dispatch. Here we use an SSSC as an example to illustrate the equivalence, and the same analysis can also apply to other FACTS controllers. The voltage-source model and the equivalent-impedance model are shown in Fig. 2(a) and (b), respectively. The term Z_{m2} denotes the equivalent impedance for the series voltage source and jX_{t2} denotes the series transformer reactance. For simplicity, the transmission line is assumed to be lossless, so the line impedance is $Z_1 = jX_1$. Therefore, the equivalent impedance can be found from the following equations:

$$\widetilde{I}_{12} = \frac{\widetilde{V}_1 - \widetilde{V}_2 - \widetilde{V}_{m2}}{j(X_{t2} + X_1)}, Z_{m2} = \frac{\widetilde{V}_{m2}}{\widetilde{I}_{12}}. \tag{23}$$

The standalone SSSC does not exchange active power with the ac system, so the voltage insertion $\widetilde{V}_{m2}$ is perpendicular to the line current $\widetilde{I}_{12}$, which implies that Z_{m2} is purely inductive or capacitive depending whether $\widetilde{V}_{m2}$ is leading or lagging with respect to $\widetilde{I}_{12}$. Then the series voltage insertion can be expressed as

$$\widetilde{V}_{m2} = V_{m2} \angle \alpha_{m2}, \alpha_{m2} = \theta_{\widetilde{I}_{12}} \pm 90^\circ \tag{24}$$

where $\theta_{\widetilde{I}_{12}}$ is the phase of the current $\widetilde{I}_{12}$. Fig. 3 shows the phase diagram of each case, assuming that $\widetilde{V}_1$ and $\widetilde{V}_2$ are fixed before and after the voltage source insertion. In Fig. 3(a), $\widetilde{V}_{m2}$ lags $\widetilde{I}_{12}$, so Z_{m2} is an equivalent capacitor inserted into the line, leading to the increase of the voltage magnitude across the line impedance $\widetilde{V}_L$ and hence increasing the power transfer. On the contrary, Fig. 3(b) shows the opposite situation, where Z_{m2} is an equivalent reactor, which reduces the line transfer capability.

B. Fast Sensitivity Algorithm Using Equivalent Impedance

As mentioned earlier, Z_{m2} can be readily computed from (23) if $\widetilde{V}_1$ and $\widetilde{V}_2$ are fixed. However, $\widetilde{V}_1$ and $\widetilde{V}_2$ will in fact vary after

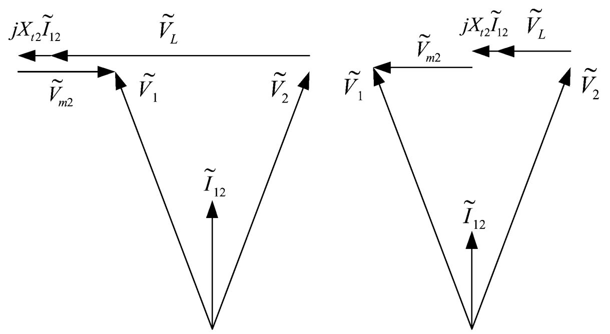

Fig. 3. Voltage-current diagram of SSSC. (a) $\widetilde{V}_{m2}$ lagging case. (b) $\widetilde{V}_{m2}$ leading case.

the series voltage source insertion. Thus the actual bus voltages are expressed as

$$\begin{aligned}\widetilde{V}_1 &= \widetilde{V}_{10} + \Delta\widetilde{V}_1 \\ \widetilde{V}_2 &= \widetilde{V}_{20} + \Delta\widetilde{V}_2\end{aligned} \tag{25}$$

where the $\widetilde{V}_{10}$ and $\widetilde{V}_{20}$ are the nominal solution, and $\Delta\widetilde{V}_1$ and $\Delta\widetilde{V}_2$ are incremental voltages due to the voltage insertion. In other words, $\Delta\widetilde{V}_1$ and $\Delta\widetilde{V}_2$ are critical for solving Z_{m2}. The following formulation is proposed to find $\Delta\widetilde{V}_1$ and $\Delta\widetilde{V}_2$.

In the base case of a N-bus system, the equation of the bus current injection is

$$\widetilde{I}_0 = Y_0\widetilde{V}_0 \tag{26}$$

where Y_0 is the bus admittance matrix without any VSC insertion and $\widetilde{V}_0$ is the nominal bus voltage solution. After the insertion of the series voltage source, the current injection equation changes to

$$\widetilde{I} = Y\widetilde{V} = (Y_0 + \Delta Y)(\widetilde{V}_0 + \Delta\widetilde{V}) \tag{27}$$

where $\Delta\widetilde{V}$ is the incremental bus voltage and ΔY accounts for the VSC insertion, which can be expressed as

$$\Delta Y = \begin{bmatrix} \Delta y_{11} & \Delta y_{12} & 0_{1,N-2} \\ \Delta y_{21} & \Delta y_{22} & 0_{1,N-2} \\ 0_{N-2,1} & 0_{N-2,1} & 0_{N-2,N-2} \end{bmatrix} \tag{28}$$

where the zeros denote zero vectors and matrices whose dimensions are indicated by the subscripts, and

$$\begin{aligned}\Delta y_{11} &= \frac{1}{jX_{t2} + Z_{m2} + jX_1} - \frac{1}{jX_1} \\ \Delta y_{22} &= \Delta y_{11}, \Delta y_{12} = \Delta y_{21} = -\Delta y_{11}.\end{aligned} \tag{29}$$

If the voltage injected by a VSC is a small perturbation we can assume the current injections into the generation and load buses are unchanged, which implies $\widetilde{I}_0 = \widetilde{I}$. Combining (26) and (27), and neglecting the second-order item $\Delta Y \Delta\widetilde{V}$, we obtain

$$\Delta\widetilde{V} = -Y_0^{-1}\Delta Y\widetilde{V}_0 \tag{30}$$

where the inversion of Y_0 is achieved via sparse LU decomposition which is computed only once.

Thus we succeed in setting up the connection between ΔV and Z_{m2}. However, both of them are unknown from the nominal solution, so it is not possible to solve for Z_{m2} directly. Therefore, an iterative algorithm is utilized to obtain the solution, using the following steps.

1) Solve the base case (excluding the series voltage source and series transformer) to get the nominal solution. Use $\widetilde{V}_{10}$ and $\widetilde{V}_{20}$ as the actual bus voltages $\widetilde{V}_1$ and $\widetilde{V}_2$.
2) Substitute $\widetilde{V}_1$ and $\widetilde{V}_2$ into (23), where $\widetilde{V}_{m2}$ is from (24) with the voltage magnitude V_{m2} equal to a small perturbation (e.g., 0.1 p.u.), to obtain the equivalent impedance Z_{m2}.
3) Compute the incremental values $\Delta\widetilde{V}_1$ and $\Delta\widetilde{V}_2$ by using (28)–(30).
4) If the change of $\Delta\widetilde{V}$ is small, the iteration has converged and $\Delta\widetilde{V}$ is the incremental change for computing the sensitivities. Otherwise, $\Delta\widetilde{V}$ is used to update $\widetilde{V}_1$ and $\widetilde{V}_2$ using (25). Then go back to Step 2 to continue the iteration.

The iterative algorithm is summarized by the flowchart in Fig. 4. The main advantage of this approach is that the base loadflow solution does not contain the FACTS controller. Hence a conventional loadflow program without FACTS controller capability can be used.

Note that (29) is derived for an SSSC. Similar equations for a UPFC and an IPFC can be found in [24].

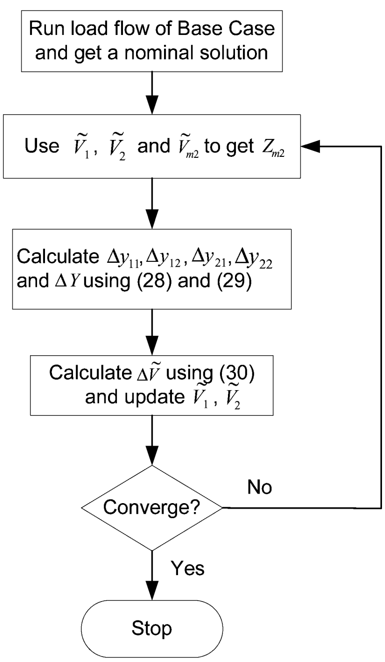

Fig. 4. Fast algorithm of equivalent impedance calculation.

TABLE I
EQUIVALENT IMPEDANCE OF DIFFERENT CONFIGURATIONS

Location	Inserted V_{m2} (pu)	Exact Z_{m2} ($\times 10^{-3}$, pu)	Approximate Z'_{m2} ($\times 10^{-3}$, pu)
SSSC in	0.1	$-j1.004$	$-j1.017$
Line 1-3	-0.1	$j1.04$	$j1.05$
SSSC in	0.1	$-j1.55$	$-j1.55$
Line 1-7	-0.1	$j1.6$	$j1.6$
SSSC in	0.1	$-j1.256$	$-j1.228$
Line 3-4	-0.1	$j1.423$	$j1.39$

C. Sensitivity Analysis Using Equivalent Impedance

To illustrate, the equivalent impedance algorithm is applied to a 1673-bus New York system with an SSSC in three possible locations: Line 1-3, Line 1-7, and Line 3-4. The values obtained from the equivalent impedance algorithm after two iterations are listed in Table I for each location, and for comparison the exact values obtained from the loadflow solution are also shown. For the inserted voltage in this table, the positive direction is defined as the one for increasing line flow and the negative one for decreasing line flow.

The results in Table I show that the algorithm can achieve less that 3% error in computing the equivalent impedance after only two iterations. As an example, for the case of an SSSC in Line 1-3, a voltage insertion of 0.1 p.u. for increasing power flow results in an equivalent impedance of $-j0.001004$ p.u. (capacitive), which will reduce the line reactance. A voltage insertion of the same amount in the opposite direction leads an equivalent impedance of $j0.00104$ p.u. (inductive) which will reduce the line flow. Note that the equivalent impedances due to these two voltage insertions are not exactly anti-symmetrical because of the transformer series reactance.

IV. APPLICATIONS

In this section, the two proposed methodologies on sensitivity analysis are applied to the 1673-bus system. In general, the dispatch variations are not linear as the setpoint of the VSC changes. However, if we are interested in a small neighborhood of an operating condition, a sensitivity analysis can be applied. Three applications are studied. The UPFC and two-SSSC configurations are utilized to redispatch the system to relieve line flow congestion, using sensitivities generated by the analytical formulation (21). The equivalent impedance approach is used to assess the siting of new FACTS controller installations at multiple locations.

A. Real-Time System Redispatch Using Series VSC Sensitivities

For an existing series VSC FACTS controller in the system, the formulation (21) can be used to compute the sensitivities of line flows due to the series VSC insertion. The following two examples demonstrate its application.

1) Line Flow Redispatch Using a UPFC: The UPFC is composed of a series VSC in Line 1-3 and a shunt VSC on Bus 1. It is used to regulate the line flows and to improve power transfer capability. Table II shows two sets of sensitivities with Line 5-3 in service and with Line 5-3 tripped, respectively. Instead of using the voltage magnitude and phase angle to indicate the series voltage insertion, we show the direct-axis (d-axis) component V_d and the quadrature-axis (q-axis) component V_q of the inserted voltage vector with respect to the from-bus angle.

TABLE II
SENSITIVITIES OF LINE POWER FLOWS ON UPFC (MW/P.U.)

Line	with Line 5-3		Line 5-3 Tripped	
	q-Axis	d-Axis	q-Axis	d-Axis
1-3	101.48	26.95	88.52	30.60
1-7	-14.55	-4.57	-16.84	-7.05
1-5	-84.56	22.76	56.97	22.75
5-6	-21.52	-5.62	-25.60	-9.13
5-3	-36.68	-7.63	N/A	N/A
6-7	-4.28	-2.11	-3.50	-2.87
7-9	-9.22	-3.20	-9.67	-4.73
6-10	-27.68	-5.41	-33.09	-9.53
10-3	-19.36	-3.70	-24.56	-6.62
10-4	-8.26	-1.51	-8.14	-2.59
3-4	29.27	9.13	39.47	14.20
15-6	-8.61	-1.59	-9.51	-2.77
5-13	-9.79	0.88	7.87	1.64

From the results in Table II, we can see that line active power is much more sensitive to V_q than V_d. Using the sensitivities, one can readily redispatch the FACTS controller setpoints to adjust the line active power flow to their desired values. For example, in contingency analysis, if Line 5-3 were tripped, the flow in Line 1-3 would increase to 719 MW from the original 541 MW. If the flow on Line 1-3 is limited to 700 MW, V_q of the series VSC should be set at $(700 - 719)/88.52 \approx -0.22$ p.u. The resulting flow on Line 1-3 would change to 699.8 MW. These results are shown in Fig. 5.

2) Line Flow Shift Using Two SSSCs: Next, we discuss the application of the two SSSCs (one in Line 1-7 and one Line 1-3) to demonstrate the line active power shift around Bus 8. In the base case, the total power flow in Lines 1-3 and 1-7 is about 916 MW, eventually supplying in part the loads. In particular, Line 8-16 is loaded to 898.2 MW [Fig. 6(a)]. Suppose the limit of secure operation on Line 8-16 is 890 MW. Thus, the objective of regulation control is to use the two SSSCs to redispatch the Line 8-16 flow to below the limit, while keeping the total power flow to the load area unchanged. The problem can be formulated as controlling 2 SSSCs to achieve

$$\begin{aligned} &\Delta P_{1-3} + \Delta P_{1-7} = 0 \\ &\Delta P_{8-16} = 890 - 898.2 = -8.2\,\mathrm{MW}. \end{aligned} \tag{31}$$

To maintain the sum of the active power flow of Lines 1-3 and 1-7, denoted by the first equation of (31), the deployment of the two SSSCs requires a positive voltage insertion (higher P) in one line and a negative voltage insertion (lower P) in the other line. The sensitivities of line flows in the two SSSCs are computed and shown in Table III. These values are similar to those observed on the actual network.

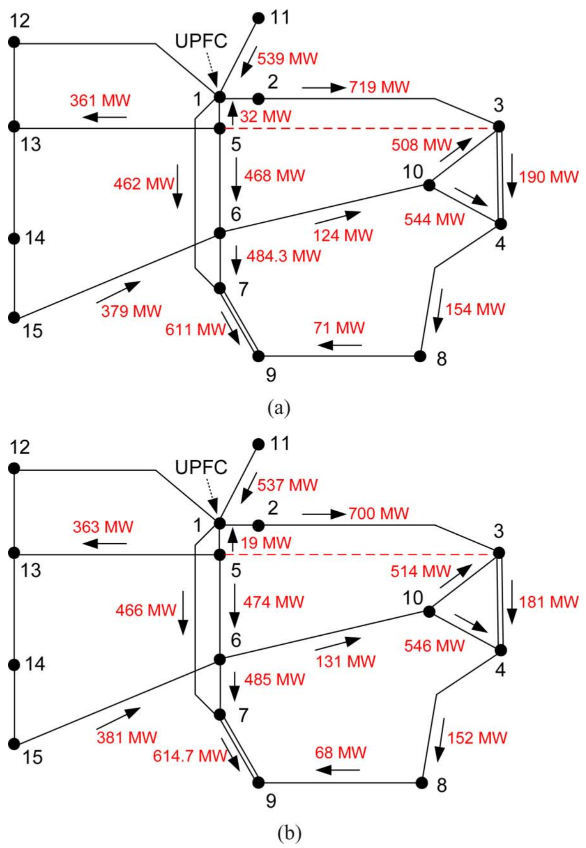

Fig. 5. System flow redispatch using sensitivity. (a) Before redispatch. (b) After redispatch with $V_q = -0.22$ p.u.

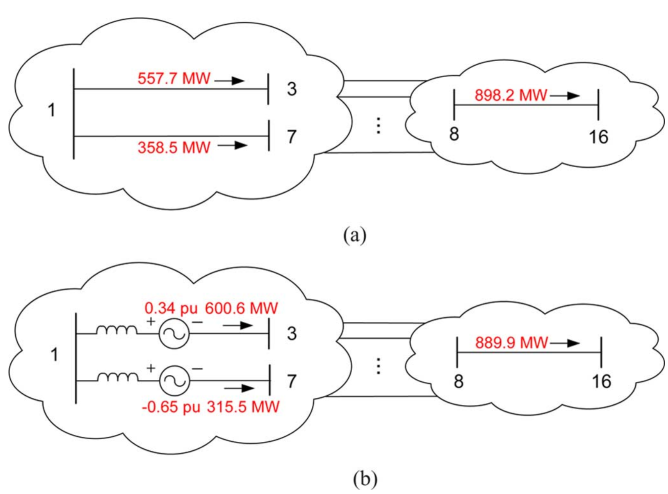

Fig. 6. Redispatch of active power in Line 8-16 using two SSSCs. (a) Before redispatch. (b) After redispatch.

TABLE III
SENSITIVITIES OF LINE POWER FLOWS ON TWO SSSCS (MW/P.U.)

Line	SSSC in Line 1-3	SSSC in Line 1-7
1-3	101.8	−12.6
1-7	−13.6	58.8
8-16	−5	10

Using the sensitivities, (31) can be expressed as

$$(101.8\Delta V_{s1} - 12.6\Delta V_{s2}) + (-13.6\Delta V_{s1} + 58.8\Delta V_{s2}) = 0$$
$$-5\Delta V_{s1} + 10\Delta V_{s2} = -8.2\,\mathrm{MW} \quad (32)$$

where ΔV_{s1} and ΔV_{s2} are the voltage insertions in Lines 1-3 and 1-7, respectively. Solving from (32), the desired deployment of the two SSSCs is

$$\Delta V_{s1} = 0.34\,\text{p.u.}, \quad \Delta V_{s2} = -0.65\,\text{p.u.} \quad (33)$$

The line flows after redispatch are shown in Fig. 6(b). After the redispatch, the total power flow of Lines 1-3 and 1-7 does not change, with about a 43 MW increase in Line 1-3 and a 43 MW reduction in Line 1-7. However, the flow in Line 8-16 is controlled to 890 MW.

B. *Optimal Location for Series VSC Installation*

The optimal siting of series VSC in the 1673-bus system using sensitivities is discussed here as a third application of sensitivity analysis. Because there are many possible locations to be considered, the equivalent impedance method would be more efficient for this application, because the Y_0 matrix (30) is constant for all locations and the ΔY matrix for the individual series VSC is sparse with only four non-zero terms. From the equivalent impedance algorithm, the incremental bus voltage $\Delta\tilde{V}$ can be computed, from which the system transfer capability can be assessed by observing the change in angular differences between the generation buses and the load buses.

In this large power system, although all the transmission lines can be regarded as candidate locations for series VSC insertion, in practice, we only consider the transmission lines in the main power transfer corridors. Thus we choose and compare the following candidate lines: 1-3, 1-7, 5-6, 5-3, 6-7, 3-4, and 6-10.

1) Maximizing the Incremental Active Power Flow on the Series VSC Compensated Line: The objective function can be formulated as

$$J_1 = \Delta P_{\mathrm{to}} \quad (34)$$

where ΔP_{to} is the incremental active power of the compensated line.

The results on using the equivalent reactance method to compute the incremental power flow on the seven candidate lines are shown in Fig. 7. It is obvious that the active power flow of Line 3-4 is most sensitive to the insertion of a series VSC.

This analysis is interesting but by itself may not be sufficient to determine the best location for a series VSC. Because increasing the flow on a series compensated line will reduce the flow in some other part of the network, a more comprehensive approach is proposed in the following.

2) Maximizing the Incremental Total Transfer Capacity: The total transfer capacity from generation to load is an important criterion of assessing the benefit of FACTS controllers. Instead of increasing the generation and load of the system simultaneously to stress the system, we can observe the change in the

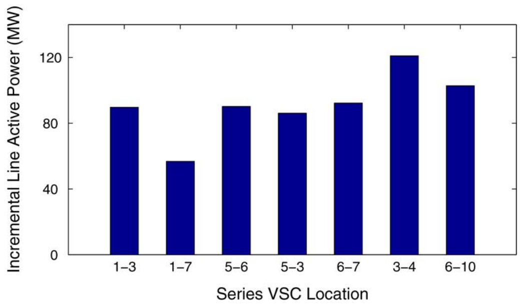

Fig. 7. Incremental line active power of different series VSC locations for a 1.0 p.u. VSC insertion.

phase angle difference between a generator bus and a load bus, with the series VSC in different locations. By reducing the phase angle difference, the series VSC strengthens the transfer path and improves the stability margin.

In this system, there are two main generation zones, whose power goes through Bus 1 to the loads. So Bus 1 can be regarded as the equivalent generation bus. The main load area is supplied through Buses 17, 18, and 19. Thus the series VSC siting problem can be selected as the location which minimizes the index

$$J_2 = w_1 \Delta\theta_{1-17} + w_2 \Delta\theta_{1-18} + w_3 \Delta\theta_{1-19} \quad (35)$$

where $\Delta\theta_{1-17}$, $\Delta\theta_{1-18}$, and $\Delta\theta_{1-19}$ are the incremental angle difference between Bus 1 and Buses 17, 18, and 19, respectively, with the series VSC compensation. The weights w_1, w_2, and w_3 are used to give preferences to different load buses and are constrained by

$$w_1 > 0, w_2 > 0, w_3 > 0, w_1 + w_2 + w_3 = 1. \quad (36)$$

The resulting decreases in the bus angle differences by using the equivalent impedance method are shown in Table IV, for a 1 p.u. series VSC voltage insertion. The series VSC in Line 1-3 results in the most decrease in angle differences between Bus 1 and all three of Buses 17, 18, and 19. Line 5-3, which parallels Line 1-3, is also a good option whereas Line 3-4 is less effective. For this system, a 1° phase angle difference between Buses 1 and 17 translates to about 120 MW increase of capacity. Thus, for rated-capacity insertion, the series VSC in Line 1-3 can help to improve the transfer by 120 MW for the whole system. This analysis confirms the actual installation of a series VSC at that location.

Sensitivity analysis is only part of a comprehensive planning process on siting of new VSC-based FACTS controllers. The example here shows how good candidate locations can be found quickly. Then other studies, such as transient and voltage stability analysis, need to be performed to further support the sizing and the cost-benefit of the new installation. Such studies can also be simplified using the results in [25] which show that when the rating of a FACTS controller is relatively small compared to the capability of a transfer path, the dynamic stability improvement due to a FACTS controller is approximately proportional to its rating.

TABLE IV
INCREMENTAL ANGLE DIFFERENCE BETWEEN THE GENERATOR AND LOAD BUSES (DEG) WITH 1 P.U. VSC INSERTION

Location	Bus 1-Bus 17	Bus 1-Bus 18	Bus 1-Bus 19
1-3	−1.15	−1.17	−1.05
1-7	−0.75	−0.78	−0.75
5-6	−0.83	−0.85	−0.81
5-3	−1.02	−1.04	−0.94
6-7	−0.70	−0.72	−0.71
3-4	−0.81	−0.83	−0.77
6-10	−0.59	−0.60	−0.49

Here we briefly summarize the computation advantages of the two proposed FACTS controller sensitivity methods. FACTS controller sensitivity was computed in an earlier paper [18] using repeated loadflow solutions. Here an analytical sensitivity formula (21) is developed, requiring only the solution of a nominal loadflow including the FACTS controller, and hence this approach is more efficient than that in [18]. However, if the FACTS controller is placed in a different location, then the analytical formula requires a new loadflow solution with the FACTS controller in the new location. On the contrary, the equivalent impedance method requires only one single loadflow solution without any FACTS controller models. The sensitivity computation is based on the same Y matrix and can be solved in a few iterations for each FACTS controller in a different location. This method is particular efficient when one needs to study the impact of FACTS controllers in many locations.

V. CONCLUSION

In this paper, we have investigated the voltage and power flow sensitivities with respect to VSC-based FACTS controllers in a large system. Two different approaches, an analytical formula based on the injected-voltage-source model and an equivalent-impedance-based method, are presented for the sensitivity analysis. These two methods are illustrated on a 1673-bus power system. The analytical formula approach is used to compute the sensitivities of line flows and then to redispatch the network flows. The equivalent impedance approach is used to investigate the optimal siting for new FACTS controller installations. The results show the application values of the proposed methods.

REFERENCES

[1] C. Schauder, M. Gernhardt, E. Stacey, T. Lemak, L. Gyugyi, T. W. Cease, and A. Edris, “TVA STATCOM project: Design, installation, and commissioning,” in *Proc. CIGRE Meeting*, Paris, France, Aug. 1996, Paper 14–106.

[2] T. Larsson, A. Petersson, A. Edris, D. Kidd, and F. Aboytes, “Eagle pass back-to-back tie: A dual purpose application of voltage source converter technology,” in *Proc. IEEE PES Summer Meeting*, Jul. 2001, vol. 3, pp. 1686–1691.

[3] K. K. Sen, “SSSC-static synchronous series compensator: Theory, modeling, and application,” *IEEE Trans. Power Del.*, vol. 13, no. 1, pp. 241–246, Jan. 1998.

[4] B. A. Renz, A. J. F. Keri, A. S. Mehraban, J. P. Kessinger, C. D. Schauder, L. Gyugyi, L. J. Kovalsky, and A.-A. Edris, “World’s first unified power flow controller on the AEP system,” in *Proc. CIGRE Meeting*, Paris, France, 1998, Paper 14–107.

[5] L. Gyugyi, K. K. Sen, and C. D. Schauder, “The interline power flow controller concept: A new approach to power flow management in transmission systems,” *IEEE Trans. Power Delivery*, vol. 4, no. 3, pp. 1115–1123, Jul. 1999.

[6] B. Fardanesh, B. Shperling, E. Uzunovic, and S. Zelingher, "Multi-converter FACTS devices: The generalized unified power flow controller (GUPFC)," in *Proc. 2000 IEEE PES Winter Power Meeting*, Jul. 2000, vol. 2, pp. 1020–1025.

[7] B. Fardanesh, M. Henderson, B. Shperling, S. Zelingher, L. Gyugyi, C. Schauder, B. Lam, J. Mountford, R. Adapa, and A. Edris, "Convertible static compensator application to the New York transmission system," in *Proc. CIGRE Meeting*, Paris, France, 1998, Paper 14–103.

[8] W. Shao and V. Vittal, "LP-based OPF for corrective FACTS control to relieve overloads and voltage violations," *IEEE Trans. Power Syst.*, vol. 21, no. 4, pp. 1832–1839, Nov. 2006.

[9] J. G. Singh, S. N. Singh, and S. C. Srivastava, "Enhancement of power system security through optimal placement of TCSC and UPFC," in *Proc. IEEE PES General Meeting*, Jun. 2007, pp. 1–6.

[10] H. Okamoto, A. Kurita, and Y. Sekine, "A method for identification of effective locations of variable impedance apparatus on enhancement of steady-state stability in large scale power systems," *IEEE Trans. Power Syst.*, vol. 10, no. 3, pp. 1401–1407, Aug. 1995.

[11] A. Berizzi, M. Delfanti, P. Marannino, M. S. Pasquadibisceglie, and A. Silvestri, "Enhanced security-constrained OPF with FACTS devices," *IEEE Trans. Power Syst.*, vol. 20, no. 3, pp. 1597–1605, Aug. 2005.

[12] T. Jibiki, E. Sakakibara, and S. Iwamoto, "Line flow sensitivities of line reactances for congestion management," in *Proc. IEEE PES General Meeting*, Jun. 2007, pp. 1–6.

[13] S. An, J. Condren, and T. W. Gedra, "An ideal transformer UPFC model, OPF first-order sensitivities, and application to screening for optimal UPFC locations," *IEEE Trans. Power Syst.*, vol. 22, no. 1, pp. 68–75, Feb. 2007.

[14] C. Canizares, Ed., Voltage Stability Assessment: Concepts, Practices and Tools, Aug. 2002, IEEE-PES PSS Subcommittee, SP101PSS.

[15] C. R. Fuerte-Esquivel and E. Acha, "Unified power flow controller: A critical comparison of Newton-Raphson UPFC algorithms in power flow studies," *Proc. Inst. Elect. Eng., Gen., Transm., Distrib.*, vol. 144, no. 5, pp. 437–444, Sep. 1997.

[16] C. R. Fuerte-Esquivel, E. Acha, and H. Ambriz-Perez, "A comprehensive Newton-Raphson UPFC model for the quadratic power flow solution of practical power networks," *IEEE Trans. Power Syst.*, vol. 15, no. 1, pp. 102–109, Feb. 2000.

[17] X.-P. Zhang, "Modelling of the interline power flow controller and the generalized unified power flow controller in Newton power flow," *Proc. Inst. Elect. Eng., Gen., Transm., Distrib.*, vol. 150, no. 3, pp. 268–274, May 2003.

[18] X. Wei, J. H. Chow, B. Fardanesh, and A.-A. Edris, "A common modeling framework of voltage-sourced converters for loadflow, sensitivity, and dispatch analysis," *IEEE Trans. Power Syst.*, vol. 19, no. 2, pp. 934–941, May 2004.

[19] D. G. Ramey, R. J. Nelson, J. Bian, and T. A. Lemak, "Use of FACTS power flow controllers to enhance transmission transfer limits," in *Proc. Amer. Power Conf.*, 1994, vol. 56I, pp. 712–718.

[20] L. Gyugyi, C. D. Schauder, and K. K. Sen, "Static synchronous series compensator: A solid-state approach to the series compensation of transmission lines," *IEEE Trans. Power Del.*, vol. 12, no. 1, pp. 406–417, Jan. 1997.

[21] S. Zelingher, B. Fardanesh, E. Uzunovic, M. Parisi, L. Hopkins, A.-A. Edris, J. Chow, X. Jiang, and X. Fang, "A novel operator training simulator for system dispatch of multi-functional FACTS controllers," in *Proc. CIGRE Meeting*, Paris, France, 2006, Paper B4-210.

[22] X. Jiang, J. H. Chow, A.-A. Edris, E. Uzunovic, B. Fardanesh, M. Parisi, and X. Wei, "An efficient tool for planning and operation of reconfigurable converter-based transmission controllers," in *Proc. 2005 IEEE PES General Meeting*, Jun. 2005, vol. 3, pp. 3081–3088.

[23] X. Jiang, X. Fang, J. H. Chow, A.-A. Edris, E. Uzunovic, M. Parisi, and L. Hopkins, "A novel approach for modeling voltage-sourced converter based FACTS controllers," *IEEE Trans. Power Del.*, vol. 23, no. 4, pp. 2591–2598, Oct. 2008.

[24] X. Fang, "Rated-capacity dispatch, sensitivity analysis, and controller design of VSC-based FACTS controllers," Ph.D. dissertation, Rensselaer Polytechnic Inst., Troy, NY, Mar. 2008.

[25] X. Jiang, J. H. Chow, A.-A. Edris, B. Fardanesh, and E. Uzunovic, "Transfer path stability enhancement by voltage-sourced converter-based facts controllers," *IEEE Trans. Power Del.*, submitted for publication.

Xinghao Fang received the B.S. and M.S. degree in electrical engineering from Tsinghua University, Beijing, China, in 2002 and 2004, respectively, and the Ph.D. degree from Rensselaer Polytechnic Institute, Troy, NY, in 2008.

He is now a Planning Engineer at the National Grid, Westborough, MA. His research interests include FACTS controller modeling, control and application in power systems, and power transmission operation and control.

Joe H. Chow received the B.S.E.E. and B.Math degrees from the University of Minnesota, Minneapolis, and the M.S. and Ph.D. degrees from the University of Illinois, Urbana.

He is a Professor of electrical, computer, and systems engineering at Rensselaer Polytechnic Institute (RPI), Troy, NY. Before joining RPI, he worked in the Power System Division of General Electric Company, Schenectady, NY. His research interests include modeling and control of power systems.

Xia Jiang received the B.S.E.E. and M.S.E.E. degrees from Tsinghua University, Beijing, China, and the Ph.D. degree in electrical engineering from Rensselaer Polytechnic Institute, Troy, NY, in 2000, 2003, and 2007, respectively.

Currently, she is working at the New York Power Authority, White Plains, NY, as a Transmission System Planning Engineer. Her research interests include power system modeling, simulation, and control.

Bruce Fardanesh received the B.S. degree in electrical engineering from Sharif University of Technology, Tehran, Iran, in 1979 and the M.S. and Doctor of Engineering degrees, both in electrical engineering, from the University of Missouri-Rolla and Cleveland State University, Cleveland, OH, in 1981 and 1985, respectively.

Since 1985, he has been teaching at Manhattan College, Riverdale, NY, where he holds the rank of Associate Professor of electrical engineering. Currently, he is working as a Senior Research and Technology Development Engineer at the New York Power Authority, White Plains, NY. His areas of interest are power system dynamics, control, and operation.

Edvina Uzunovic received the B.S.E.E. degree from the University of Sarajevo, Sarajevo, the former Yugoslav Republic, in 1990. After professional positions in Sarajevo, she joined the Department of Electrical and Computer Engineering at the University of Waterloo, Waterloo, ON, Canada, as a graduate student in 1993, where she received the M.A.Sc. degree in 1995 and the Ph.D. degree in 2001.

In 1999, she joined the New York Power Authority, White Plains, NY, as a Research and Technology Development Engineer. Her areas of interest are high power electronics controllers as well as stability and control of ac/dc power systems. She is a Senior Quantitative Analyst with Alliant Energy.

Abdel-Aty Edris received the B.S. degree with honors from Cairo University, Cairo, Egypt, the M.S. degree from Ein-Shams University, Cairo, and the Ph.D. degree from Chalmers University of Technology, Gothenborg, Sweden.

He was a Technical Leader of Transmission and Substation Asset Utilization Target of the Science and Technology Division, EPRI, Palo Alto, CA. Before joining EPRI, he was with ABB, Vasteras, Sweden, and the U.S. working on development of reactive power compensation and high voltage dc transmission systems. He is now with Siemens-PTI, San Jose, CA.

Dr. Edris is a member of several IEEE and CIGRE Working Groups. He is the recipient of the 2006 IEEE FACTS Awards.